JACS
JOURNAL OF THE AMERICAN CHEMICAL SOCIETY
Article
pubs.acs.org/JACS

Efficient and Limiting Reactions in Aqueous Light-Induced Hydrogen Evolution Systems using Molecular Catalysts and Quantum Dots

Carolina Gimbert-Suriñach,[†,⊥] Josep Albero,[†,⊥] Thibaut Stoll,[†] Jérôme Fortage,[§] Marie-Noëlle Collomb,[§] Alain Deronzier,[§] Emilio Palomares,*[,†,‡] and Antoni Llobet*[,†,∥]

[†]Institute of Chemical Research of Catalonia (ICIQ), Avinguda Països Catalans 16, 43007 Tarragona, Spain
[§]Département de Chimie Moléculaire, UMR 5250, Institut de Chimie Moléculaire de Grenoble, FR-CNRS-2607, Laboratoire de Chimie Inorganique Rédox, Université Joseph Fourier Grenoble 1/CNRS, BP 53, 38041 Grenoble cedex 9, France
[‡]Institució Catalana de Recerca i Estudis Avançats (ICREA), Passeig Lluís Companys 23, 08010 Barcelona, Spain
[∥]Departament de Química, Universitat Autònoma de Barcelona (UAB), 08193 Cerdanyola del Vallès, Barcelona, Spain

Supporting Information

ABSTRACT: Hydrogen produced from water and solar energy holds much promise for decreasing the fossil fuel dependence. It has recently been proven that the use of quantum dots as light harvesters in combination with catalysts is a valuable strategy to obtain photogenerated hydrogen. However, the light to hydrogen conversion efficiency of these systems is reported to be lower than 40%. The low conversion efficiency is mainly due to losses occurring at the different interfacial charge-transfer reactions taking place in the multicomponent system during illumination. In this work we have analyzed all the involved reactions in the hydrogen evolution catalysis of a model system composed of CdTe quantum dots, a molecular cobalt catalyst and vitamin C as sacrificial electron donor. The results demonstrate that the electron transfer from the quantum dots to the catalyst occurs fast enough and efficiently (nanosecond time scale), while the back electron transfer and catalysis are much slower (millisecond and microsecond time scales). Further improvements of the photodriven proton reduction should focus on the catalytic rate enhancement, which should be at least in the hundreds of nanoseconds time scale.

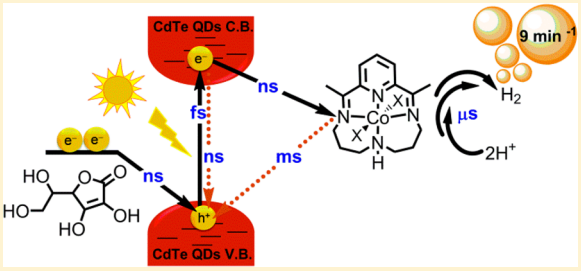

INTRODUCTION

Efficient and cost-effective production of hydrogen gas from water using sunlight as the ultimate energy source is one of the major challenges for researchers in the 21st century. In recent years, promising results have been reported using semiconductor materials for the photodriven hydrogen production.[1−10] When a semiconductor material is irradiated by light with energy higher than its optical band gap (BG), an electron of the valence band (VB) is promoted to the conduction band (CB) leaving a hole in the VB. Subsequently, the electrons and holes migrate to the surface of the semiconductor where they can be used for the reduction of protons and the corresponding oxidation process, respectively (black arrows in Figure 1). However, a major drawback of these systems is that the semiconductor photocatalytic activity is limited by undesired radiative and nonradiative recombination processes that occur in the semiconductor crystal lattice competing directly with the charge migration and the catalytic process (red arrows in Figure 1).

One strategy to improve the photocatalytic activity of semiconductors is to use a co-catalyst such as metallic platinum or rhodium, often incorporated in the crystal lattice of the semiconductor as "dopants". The co-catalyst not only lowers the activation energy for proton reduction but also acts as an electron trap and favors charge separation. The overall result is an increase of the driving force toward the formation of hydrogen, reducing the kinetic competition with the charge recombination processes.[8,9] On the other hand, the so-called molecular approaches for hydrogen production have been attracting much interest since the hydrogen production yields can be substantially higher due to the versatility and tunability offered by the coordinating ligands. These systems, analogously to the photosynthetic systems in plants, algae, and some bacteria, separate the light absorption structural unit from the molecular catalytic site.[7,11]

A recent elegant approach that combines both strategies mentioned before has been recently reported.[3,10] They describe the photogeneration of hydrogen in water by employing semiconductor CdSe nanocrystals as light harvesting materials,[12−14] with the subsequent electron transfer to a nickel catalyst for the concomitant reduction of protons to hydrogen. Further examples of molecular approaches using quantum dots (abbreviated as "QD") as photosensitizers in pure water involve the use of hydrogenases and their functional mimics.[2,9,15−18] Yet, although the catalytic activity of some of these examples is

Received: February 12, 2014
Published: May 5, 2014

   dx.doi.org/10.1021/ja501489h | J. Am. Chem. Soc. 2014, 136, 7655−7661

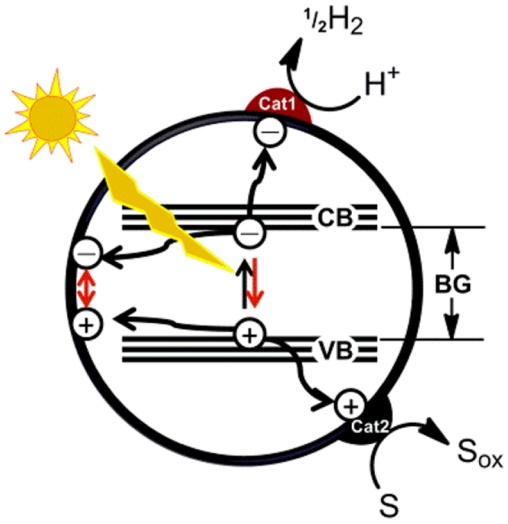

Figure 1. Schematic representation of photodriven hydrogen generation at a semiconductor. Black Arrows: Light excitation, charge migration (electrons = ⊖, holes = ⊕) and catalytic reactions. Red Arrows: photoluminescence and charge recombination. CB = conduction band, VB = valence band, BG = band gap. S/Sox = substrate/oxidized substrate. Cat1 = catalyst for water reduction. Cat2 = catalyst for substrate oxidation.

remarkably high (up to hundreds of thousands of turnover numbers), the reported quantum yields are still below 40% even when using monochromatic light. In this context, a deeper knowledge of the kinetics of both charge transfer and bond formation/breaking are the keys to understand the limitations of photodriven hydrogen evolving systems based on molecular approaches.[19−21] Herein, we take advantage of a highly active system composed of QDs and a cobalt molecular catalyst to study the kinetics involved in the overall photo-induced catalytic process. We selected the components based on the following requirements: (1) a light harvesting unit that absorbs in the visible light region; (2) a molecular water reduction catalyst with a well-defined structure; and (3) the whole system has to work in purely aqueous conditions.

Water-soluble CdTe QDs are excellent photosensitizing candidates as they have high extinction coefficients and offer the intrinsic advantages of semiconductor-based nanocrystals such as high photoluminescence quantum yields and quantum confinement effects.[12−14] As catalyst, we selected the macrocyclic cobalt complex Co(III)-**1** in Chart 1 because of its great stability and activity for hydrogen production in water.[22,23] Our results show that the catalytic activity of Co(III)-**1** is superior to that of the cobaloxime-type catalyst Co(III)-**2**, that has also been used as proton reduction catalyst in water (Chart 1).[24] An aqueous equimolar mixture of ascorbic acid/sodium ascorbate (H_2A/NaHA) was chosen as both buffer and sacrificial electron donor to trap the photogenerated holes in the CdTe QDs.

A detailed study of the thermodynamics and kinetics of the system based on the components depicted in Chart 1 has allowed us to build a complete energetics−kinetics scheme of the proton reduction catalysis and identify what are the major advantages and limitations in this kind of photodriven hydrogen evolution processes.

RESULTS

Electron Transfer From CdTe QD to the Cobalt Catalyst. Upon light absorption by the CdTe QD, the excited electron in the CB of the quantum dot is transferred to the cobalt catalyst so that it can start the catalytic proton reduction sequence (Scheme 1). This step is an oxidative quenching of the excited QD (QD*) by the cobalt catalyst. Two consecutive electron-transfer reactions are necessary to generate the Co(I) active species from complexes Co(III)-**1** or Co(III)-**2**.[22−26] The reduction potentials for the couples E_{pc} = Co(III)/Co(II) and $E_{1/2}$ = Co(II)/Co(I) were measured and are given in Scheme 1 (see also Figure S1). We measured the energy of the CB of our CdTe QDs and obtained an approximate value of −1.2 V vs NHE (Figure S2), and therefore both electron-transfer reactions are thermodynamically favorable. In the case of complex **1**, the initial oxidation state of the cobalt at the beginning of the catalysis is Co(II) since the Co(III)-**1** species is reduced by H_2A (see UV−vis spectra in Figure S3).[22] Nevertheless, the oxidized species Co(III)-**1** can be formed during hydrogen evolution turnover (Scheme 1).

Chart 1. Components of the Catalytic System Studied in This Work[a]

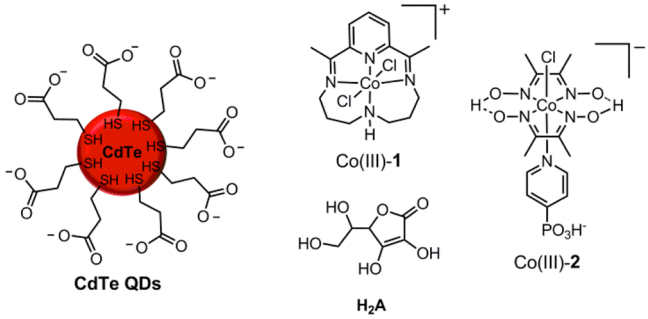

[a]QD = quantum dot, Co(III)-**1** and Co(III)-**2** = hydrogen evolving catalysts, H_2A = ascorbic acid.

Scheme 1. Relevant Processes Towards Photodriven Hydrogen Evolution[a]

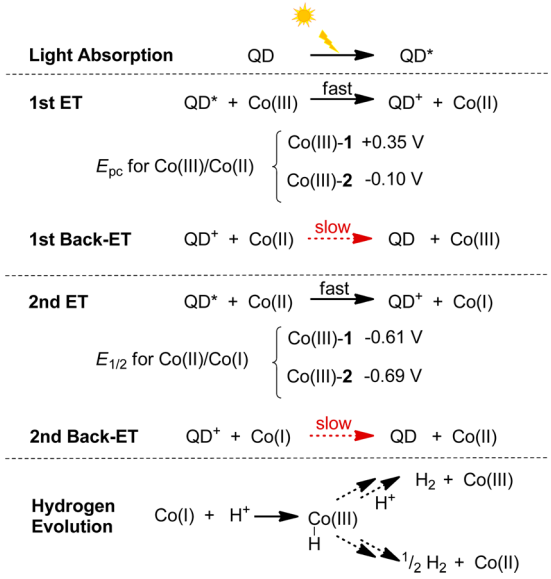

[a]Black arrows: light absorption, electron transfer (ET), and hydrogen evolution. Red arrows: back electron-transfer reactions (back-ET). Reduction potentials E_{pc} = Co(III)/Co(II) and thermodynamic reduction potentials $E_{1/2}$ = Co(II)/Co(I) are given vs NHE.

dx.doi.org/10.1021/ja501489h | J. Am. Chem. Soc. 2014, 136, 7655−7661

The first electron transfer yield from the QD CB to complex Co(III)-**1** or Co(III)-**2** has been investigated by means of steady-state fluorescence quenching experiments of binary mixtures of the QD and the molecular catalyst (Figures 2a, S4, and S5). At the same concentration, the electron transfer yield observed in the case of complex Co(III)-**1** (>90%) is significantly higher than that of complex Co(III)-**2** (50%) as illustrated in Figure 2a (compare black and red traces). Nevertheless, by increasing the amount of Co(III)-**2** considerably, it was possible to reach electron transfer yields higher than 95% (Figure S5). These results indicate that the first electron transfer in Scheme 1 is favorable for both complexes Co(III)-**1** and Co(III)-**2**.

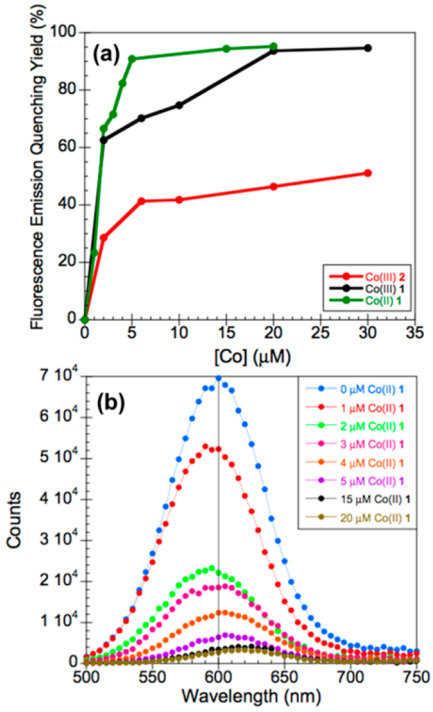

Figure 2. (a) Quenching emission yield as a function of complex concentration. (b) Steady-state photoluminescence of colloidal CdTe QDs upon addition of increasing amounts of Co(II)-**1**. The samples were excited at λ_{ex} = 405 nm. [CdTe QDs] = 2 μM.[28]

In order to perform the same study for the second electron transfer, a reduced form of complex Co(III)-**1**, that is, Co(II)-**1** was generated electrochemically and added to colloidal QDs under nitrogen to avoid oxidation to Co(III). As depicted in Figure 2 quenching of the QDs photoluminescence was higher than 95% at a concentration of [Co(II)-**1**] = 15 μM, that is, 7.5 equiv of Co(II) per mole of QDs. Unfortunately, it was not possible to perform this study for the electro-generated reduced form of complex Co(III)-**2** due to the instability of the Co(II)-**2** species during long experiment times.

Furthermore, the QDs emission lifetime was analyzed in order to evaluate the first and second electron-transfer kinetics from the QDs excited states to the different cobalt species (Figure 3). The first electron transfer is comparable and in the nanosecond (ns) time scale for both complexes Co(III)-**1** and Co(III)-**2**, but at high concentration ([Co(III)] > 10 μM) the electron transfer becomes faster for Co(III)-**1**, while that of Co(III)-**2** remains unchanged (compare black and red traces in Figure 3a). On the other hand, the second electron transfer to

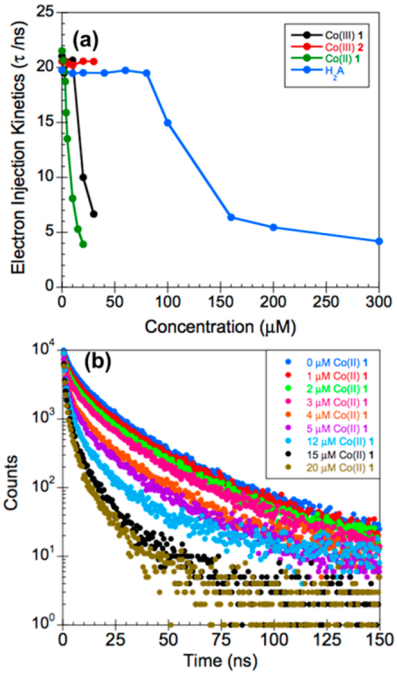

Figure 3. (a) Electron-transfer lifetime as a function of the cobalt complex and H_2A concentration. The electron-transfer lifetime was calculated following a reported methodology.[27] (b) Time-resolved photoluminescence of colloidal CdTe QDs upon addition of increasing amounts of Co(II)-**1**. The samples were excited at λ_{ex} = 405 nm and monitored at λ_{em} = 600 nm. [CdTe QDs] = 2 μM.[28]

the Co(II)-**1** species resulted to be faster (<5 ns) than that of Co(III)-**1** (≈ 10 ns) at the same concentration (compare black and green traces in Figure 3a), indicating that the second charge-transfer reaction in Scheme 1 is kinetically more favored than the first one.

Electron Transfer From HA^- to CdTe QD. Two other charge-transfer reactions that are essential for the catalysis are (i) hole transfer from the excited QD (QD*) to HA^- and (ii) reduction of oxidized QD (QD^+) by HA^-, regenerating the initial QD. In both cases, HA^- injects an electron into the QDs VB which possesses a hole. The oxidation potential of HA^- is $E_{p,a}$ = +0.36 V vs NHE,[11] and therefore the electron transfer to the QD VB (ca. 0.94 V vs NHE, Figure S2) is thermodynamically favored for both processes. Figure S6 shows the photoluminescence quenching of a QDs solution upon addition of HA^-, which is due to hole transfer from QD* to HA^-. It reaches values of electron injection yield higher than 95% at [HA^-] = 300 μM, that is, 150 equiv of HA^- per mole of QDs. The kinetics of the process has been calculated and is comparable to that of the electron transfer from QD* to Co(II)-**1** (compare blue and green traces in Figure 3a). It is worth noticing that higher amounts of HA^- than Co(II)-**1** are needed to completely quench the nanocrystals emission (150 and 10 equiv, respectively). However, the hydrogen evolution catalytic experiments are performed using a large excess of the hole scavenger (>1500 equiv, see below), and the kinetics of the hole transfer from QD* to HA^- is expected to be much faster in such conditions.

Back-Electron Transfer from Cobalt Catalyst to CdTe QD. All the results presented above show that electron transfer from the QD to the cobalt center and hole transfer from the QD to the HA^- are both kinetically and thermodynamically favored. However, undesirable back electron transfer (back-ET)

dx.doi.org/10.1021/ja501489h | J. Am. Chem. Soc. 2014, 136, 7655−7661

reactions can take place at the same time and need to be taken into account when the whole system is assessed (red arrows in Scheme 1). We have studied these recombination processes using laser transient absorption spectroscopy (L-TAS).

The transient spectra of a QDs solution containing Co(III)-**1** or Co(III)-**2**, monitored at 10 μs after excitation, show a negative signal that matches the steady-state absorption of the QDs, and therefore it can be assigned to the 1S ground-state bleaching of the nanocrystals (Figure S7). A positive signal expanding from 620 to 900 nm also appears and is similar to that observed in recent works for species derived from analogous CdTe QDs.[29,30] The transient absorption spectrum obtained by adding the reduced Co(II)-**1** species to a QDs solution did not present any significant change compared to those obtained when Co(III)-**1** or Co(III)-**2** was added. On the other hand, no signal was found at the studied time range (μs–ms) in the absence of cobalt complex, indicating that the transient signal arises from the photo-induced charge transfer between the QD and the cobalt species (Figure S7).

Taking into account that the reduced Co(II)-**1** species derived from the first charge-transfer process does not significantly absorb beyond 650 nm (Figure S3) and also the fact that the extinction coefficient of the QDs are at least 10 times higher than that of the cobalt species, we can attribute the positive signal in the transient spectra to the oxidized QD (QD^+).

The transient decays of the QD^+ were recorded and fitted to a power law function, eq 1, obtaining recombination half-lifetimes $\tau_{1/2}$ = 9.6 and 5.1 ms (ms) for Co(III)-**1** and Co(III)-**2**, respectively (Figure S7). This result indicates the formation of long-lived QD^+ after first electron transfer. In other words, the back electron transfer (back-ET) from the generated Co(II) species to the oxidized QD is slow, that is, in the millisecond time scale.

$$f(t) = A \cdot t^{\tau} \quad (1)$$

Analogous transient decay experiments using a mixture of QDs and Co(II)-**1** presented a long half-lifetime ($\tau_{1/2}$= 4.5 ms) for the QD^+ species and showed identical recombination dynamics alike Co(III)-**1** (compare green and black traces in Figure 4a).

We have already pointed out the importance of the electron transfer from the sacrificial electron donor H_2A to the QDs VB. Transient decay experiments were done with mixtures containing QDs, Co(II)-**1**, and H_2A, before and after addition of H_2A (Figure 4b). It was found that the decay of the new formed transient signal becomes 1 order of magnitude faster after addition of H_2A, that is, $\tau_{1/2}$ = 0.45 ms vs $\tau_{1/2}$= 4.5 ms, indicative for a second process taking place in the mixture and therefore supporting fast electron injection to the QDs VB by H_2A.

Hydrogen Evolution Catalysis. The rate of the catalytic proton reduction process using Co(III)-**1** has been measured electrochemically by using the foot of the wave method developed by Savéant[31] obtaining a value in the microsecond time scale, which is in agreement with other reported values in the literature (Figure S8).[26] These kinetics values are compatible to all the kinetic processes described previously and therefore encouraged us to carry out bulk experiments to evaluate the potential of the system.

Figure 5 shows the profile of hydrogen generation upon time using the hybrid CdTe QDs/Co(III)-**1** system. The rate of the catalysis depends on the concentration of the H_2A/NaHA buffer, and under optimum conditions it reaches 650 TON_{Co} in 1.5 h with a maximum turnover frequency ($TOF_{Co,max}$) of 9 min^{-1} (green trace, Figure 5). This $TOF_{Co,max}$ value is one of the highest reported using QDs as photosensitizers and a molecular catalyst in water that has not been generated *in situ*, together with two recent reports that use CdSe QDs and diiron

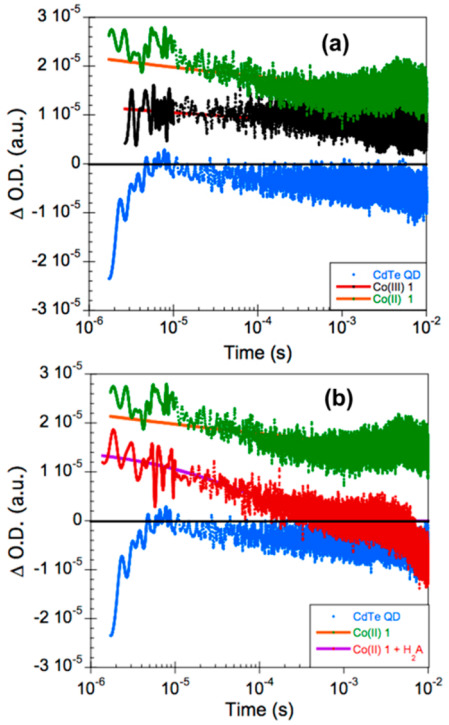

Figure 4. Transient absorption decays of colloidal CdTe QDs (a) upon addition of 30 μM of Co(III)-**1** or Co(II)-**1** and (b) upon addition of 30 μM of Co(II)-**1** and 250 μM of H_2A. The samples were excited at λ_{ex} = 430 nm, and the decays were monitored at λ_{probe} = 675 nm. [CdTe QDs] = 2 μM.[28] The orange, red, and purple lines in the plots indicate the experimental points' trend that was obtained by fitting the data to the power law function indicated in eq 1.

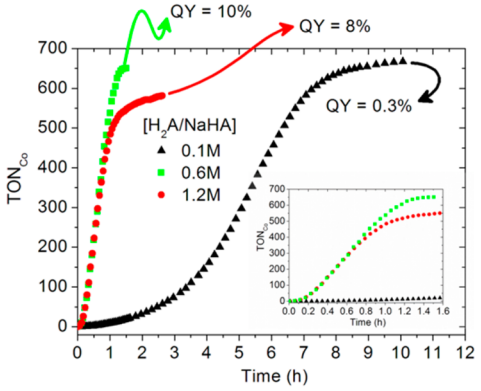

Figure 5. Photocatalytic hydrogen production experiments were performed using an aqueous mixture of [CdTe QDs] = 5.9 × 10^{-5} M, [Co(III)-**1**] = 7.5 × 10^{-5} M, and [H_2A/NaHA] = 0.1 M (▲), 0.6 M (green ■) or 1.2 M (red ●), pH = 4.1, volume = 1.5 mL, under 1 sun irradiation (λ > 400 nm). Inset: expanded graph (0–1.6 h). TON_{Co} = mol H_2/mol cobalt, average of two different replicates (within 5–10% error, see also Figure S9). Values of QY for each experiment are given at maximum conversion time and were calculated as QY = [2 × (molecules of H_2)]/[photons absorbed × Δt × area], see also Figure S10.

dx.doi.org/10.1021/ja501489h | J. Am. Chem. Soc. 2014, 136, 7655–7661

or nickel catalysts.[9,10] Other related systems with high catalytic activity are active only in organic solvents[19] or they use inorganic salts as precursors of the catalyst.[3,8] Blank experiments were performed in the absence of catalyst Co(III)-**1** and in the dark, and we did not observe the formation of significant amount of hydrogen. Interestingly, analogous catalytic tests using complex Co(III)-**2** did not produce significant amount of hydrogen as shown in Figure S9. The low stability of cobaloxime-type catalysts under acidic aqueous conditions is well-known and could explain why the catalysis using Co(III)-**2** was unsuccessful.

The quantum yield (QY) as defined in eq 2 was calculated to be 10% for the best experiment (see Figures 5 and S10). This value is similar to those obtained with related photocatalytic systems that use cobalt molecular catalysts in water[32−34] or QD with other metallic catalysts.[3,11]

$$\mathrm{QY} = \frac{2 \times (\text{molecules of } \mathrm{H_2})_{(t)}}{\text{photons absorbed} \times \Delta t \times \text{area}} \qquad (2)$$

DISCUSSION

From the combination of experiments reported in the previous section a general picture emerges of how the system "QDs molecular catalyst" manages to carry out the photo-induced reduction of water to hydrogen. The detailed description of all these experiments allowed the generation of a schematic summary of the kinetics and thermodynamics of all the significant reactions involved in this complex system, which is offered in Scheme 2.

Scheme 2. Energetics and Kinetics Scheme for the Photocatalytic Hydrogen-Evolving System Based on CdTe QDs, Cobalt Molecular Catalyst Co(III)-1, and Ascorbic Acid/Sodium Ascorbate (H_2A/NaHA)[a]

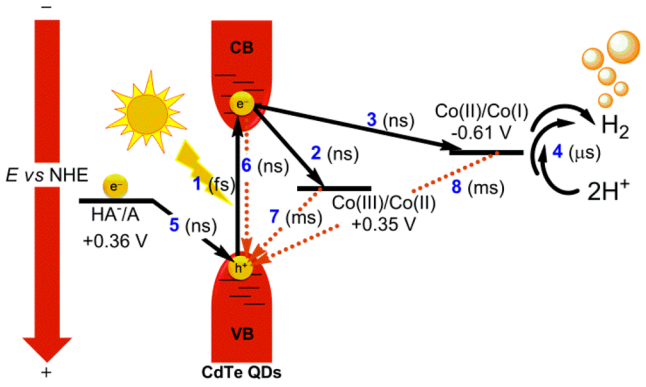

[a]A = oxidized ascorbate. Black arrows indicate favorable processes toward efficient and fast catalysis, while red arrows illustrate the undesired photoluminescence and back-electron reactions. In parentheses, the kinetics time scales are given in milliseconds (ms), microseconds (μs), or nanoseconds (ns).

The first requirement is the presence of an efficient light harvesting material such as the CdTe QDs, that are known to interact with light very fast, that is, in the femtosecond time scale (1, Scheme 2), generating a powerful reducing agent; its CB is situated at ca. $E = -1.2$ V vs NHE. Such a low redox potential will enable a large thermodynamic driving force with regards to the reduction of most relevant molecular hydrogen-evolving catalysts.[11,35,36] However, the latter reaction will only proceed if the excited QD (QD*) is sufficiently long-lived. Under our system conditions we found this excited state to be of ca. 20 ns (6, Scheme 2). Therefore, for a successful system, it is imperative that the reactions coupled to this excited state are not only thermodynamically favored but also faster than 20 ns.

We have chosen the cobalt complexes **1** and **2**, in oxidation state +3 as proton reduction catalysts. To be able to generate hydrogen they need to be reduced all the way to Co(I) via sequential two one-electron-transfer processes as indicated in Scheme 1, where their relevant redox potentials are also indicated. In all cases the thermodynamic driving force of the electron transfers to generate the corresponding Co(I) catalytically active species is huge; e.g. $\Delta E = -1.55$ and -0.59 V for the Co(III/II) and the Co(II/I) couples respectively for **1**. To evaluate the kinetics of these processes we carried out photoluminesce quenching experiments giving life times of 10 and 5 ns for the reactions indicated in arrows 2 and 3 in Scheme 2, respectively.

It is worth noticing that these experiments do not differentiate between hole transfer or electron transfer. Cyclic voltammetry experiments of Co(III)-**1** and QD show that the oxidation of Co(III)-**1** by the QD is not thermodynamically possible, and therefore the first process can unequivocally be assigned to electron transfer from the QD CB to the cobalt catalyst (Figures S1 and S2). On the other hand, assigning the second charge transfer from excited QD (QD*) to Co(II) was not trivial, as it could well be due to hole transfer from the QD VB to Co(II) to give the Co(III) species and the hypothetical reduced QD (QD^-). If this was the case, the newly formed Co(III) species would be reduced back to Co(II) by the QD^- within a few nanoseconds as just commented above. L-TAS experiments discussed in detail below showed the formation of a long-lived transient species (milliseconds). If hole transfer from QD* to Co(II) took place, this would be faster than our L-TAS instrument response (microseconds), and no L-TAS signal would be found. Therefore, the second charge-transfer process can be attributed to the second electron transfer from QD* to Co(II) to give Co(I) (3 in Scheme 2). Interestingly, the reaction between QD* and Co(II), with lower driving force, has faster kinetics than the reaction between QD* and Co(III) (5 vs 10 ns, respectively). This can be attributed to the electronic structure of Co(III) that has a low-spin $(d\pi)^6$ electronic configuration, and therefore the coming electron has to be accommodated in a $(d\sigma)$ orbital generating a high-spin d^7 complex. An additional reason why the first reduction of Co(III) is slower might be due to the huge driving force of this reaction ($\Delta E = -1.55$ V). In a recent work, the dependence of the photocatalytic hydrogen evolution rate on the ΔE using CdSe nanocrystals of different sizes has been studied. It was shown that in the range of ΔE from -0.5 to -0.8 V the system works under normal Marcus theory regime.[37] In the present case, ΔE for the first electron transfer is twice the lower limit of the range that they study, and therefore it is plausible to think that we are in the Marcus inverted region, where the first electron transfer with higher driving force is expected to have a slower rate.

The large thermodynamic driving force for the desired forward reaction is expected to generate slower back-ET reactions to the QD*, however, recombination reactions could still potentially occur with the oxidized QD^+. This is a crucial point especially if the back-ET to QD^+ is fast, in which case the cobalt catalyst will not be long-lived enough to be able to interact with protons and generate hydrogen.

dx.doi.org/10.1021/ja501489h | J. Am. Chem. Soc. 2014, 136, 7655−7661

L-TAS experiments were used to calculate the back-ET kinetics indicated by arrows 7 and 8 in Scheme 2, and we obtained values of 9.6 and 4.5 ms, respectively. The L-TAS experiment was repeated in the presence of H_2A showing a decrease of the lifetime of the transient species by 1 order of magnitude. This result is very important because it shows that the electron transfer from HA^- to the QD VB is more efficient than that of the Co(I) complex to QD^+ and thus prevents a nonproductive Co-centered reaction. Furthermore, we could also show that HA^- is capable of reductively quench the QD* by replenishing its VB in the nanosecond time scale thus avoiding the presence of the oxidizing QD^+ species (5, Scheme 2). It is remarkable that these recombination processes from reduced cobalt catalyst to oxidized quantum dot are 5−6 orders of magnitude slower (milliseconds) than the measured photo-induced electron-transfer dynamics from QD to Co catalyst (nanoseconds).

Electrochemical experiments in water, under comparable working conditions, show that the lifetime of the catalytic cycle that generates hydrogen occurs in the microsecond time scale, indicating that this system has a good match with the reactions discussed above (4, Scheme 2). Indeed upon shining light to our QDs-Co catalyst system in the presence of H_2A/NaHA generates an impressive amount of H_2 with a $TOF_{Co,max}$ of 9 min^{-1} that is among the highest ever reported in water. The ratio of hole scavenger/QD used for the hydrogen evolution experiments is 1 order of magnitude higher than that used for the photophysical experiments (>1500 vs 150, respectively), and therefore the electron transfer from the HA^- to the QDs VB is faster under catalytic conditions, hindering the formation of QD^+ and favoring the proton reduction process.

The overall picture we have managed to generate for the photocatalytically induced reduction of water, shown in Scheme 2, also allowed us to identify the limitations and the potential improvements of the present system. Thus, the main efforts need to be directed toward the minimization of unproductive reactions shown in red, in Scheme 2.

Ideally it would be desirable to be able to lower the rate of the QD* recombination reaction (6, Scheme 2) so that more light efficient systems could be generated. Alternatively, catalysts that would react faster with QD* (2 and 3, Scheme 2) would also increase the overall performance of the catalysis.

Another important improvement to the system would be the use of complexes capable of catalytically cycling faster than the microsecond time scale, avoiding unwanted competing recombination reactions such as the one shown in arrows 7 and 8 in Scheme 2.

As just discussed, the molecular catalyst plays one of the crucial roles in these systems since its interactions with the QD and with protons determine the success of the photocatalytic reaction. Indeed, it is surprising to see that when replacing catalyst **1** by **2** under the same conditions, the system practically did not yield any hydrogen, due to either catalyst decomposition in water[22,23,32] or slow electron-transfer processes.[21] The macrocyclic nature of the ligand in **1** not only makes the catalyst more robust but also could contribute to the stabilization of the Co(I) species that is formed during catalyst turnover. In this context, molecular catalysts have the potential to dramatically improve the performance of this type of systems given the large versatility of ligands that can be used to tune the electronic and structural properties at the metal center.[11,35,36]

CONCLUSION

In conclusion, we have managed to fully identify for the first time the thermodynamics and kinetics involved in a hybrid system made of CdTe QDs material and a molecular cobalt catalyst, that coupled together are an efficient light-induced proton reduction system in water. This in turn allowed us to identify which reactions need to be improved in order to come up with even better systems. Furthermore, the molecular nature of the catalysts provides a wide avenue of potential improvements given the large versatility of potential ligands that can be used.

ASSOCIATED CONTENT

Supporting Information

Additional kinetic and spectroscopic data as well as experimental details of the synthesis of CdTe QDs, Co(III)-**1**, Co(II)-**1**, and Co(III)-**2**, electrochemical procedures and photochemical hydrogen evolution experiments. This material is available free of charge via the Internet at http://pubs.acs.org.

AUTHOR INFORMATION

Corresponding Authors

allobet@iciq.es
epalomares@iciq.es

Author Contributions

⊥These authors contributed equally.

Notes

The authors declare no competing financial interest.

ACKNOWLEDGMENTS

This work was supported by MICINN (CTQ2013-49075-R), "La Caixa" Foundation, European Research Council starting Grant ERCstg-POLYDOT and the LABEX program ARCANE of Grenoble (Grant no. ANR-11-LABX-0003-01) (H2Photocat). E.P. also thanks the ICIQ, ICREA, GenCat (Project 2009 SRD 207) and MICINN (CTQ-2007-60746-BQU) for funding. C.G.S. is grateful to GenCat for a "Beatriu de Pinós" postdoctoral grant.

REFERENCES

(1) Chen, X.; Shen, S.; Guo, L.; Mao, S. S. *Chem. Rev.* **2010**, *110*, 6503.
(2) Wang, F.; Wang, W.-G.; Wang, X.-J.; Wang, H.-Y.; Tung, C.-H.; Wu, L.-Z. *Angew. Chem., Int. Ed.* **2011**, *50*, 3193.
(3) Han, Z.; Qiu, F.; Eisenberg, R.; Holland, P. L.; Krauss, T. D. *Science* **2012**, *338*, 1321.
(4) Woolerton, T. W.; Sheard, S.; Chaudhary, Y. S.; Armstrong, F. A. *Energy Environ. Sci.* **2012**, *5*, 7470.
(5) Tran, P. D.; Wong, L. H.; Barber, J.; Loo, J. S. C. *Energy Environ. Sci.* **2012**, *5*, 5902.
(6) Zhu, H.; Song, N.; Lv, H.; Hill, C. L.; Lian, T. *J. Am. Chem. Soc.* **2012**, *134*, 11701.
(7) Wen, F.; Li, C. *Acc. Chem. Res.* **2013**, *46*, 2355.
(8) Li, Z.-J.; Li, X.-B.; Wang, J.-J.; Yu, S.; Li, C.-B.; Tung, C.-H.; Wu, L.-Z. *Energy Environ. Sci.* **2013**, *6*, 465.
(9) Li, C.-B.; Li, Z.-J.; Yu, S.; Wang, G.-X.; Wang, F.; Meng, Q.-Y.; Chen, B.; Feng, K.; Tung, C.-H.; Wu, L.-Z. *Energy Environ. Sci.* **2013**, *6*, 2597.
(10) Das, A.; Han, Z. J.; Haghighi, M. G.; Eisenberg, R. *Proc. Natl. Acad. Sci. U.S.A.* **2013**, *110*, 16716.
(11) Eckenhoff, W. T.; Eisenberg, R. *Dalton Trans.* **2012**, *41*, 13004.
(12) Zhang, H.; Zhou, Z.; Yang, B.; Gao, M. *J. Phys. Chem. B* **2003**, *107*, 8.

(13) Shi, L.; Hernandez, B.; Selke, M. *J. Am. Chem. Soc.* **2006**, *128*, 6278.
(14) Gaponik, N.; Talapin, D. V.; Rogach, A. L.; Hoppe, K.; Shevchenko, E. V.; Kornowski, A.; Eychmüller, A.; Weller, H. *J. Phys. Chem. B* **2002**, *106*, 7177.
(15) Brown, K. A.; Dayal, S.; Ai, X.; Rumbles, G.; King, P. W. *J. Am. Chem. Soc.* **2010**, *132*, 9672.
(16) Brown, K. A.; Wilker, M. B.; Boehm, M.; Dukovic, G.; King, P. W. *J. Am. Chem. Soc.* **2012**, *134*, 5627.
(17) Greene, B. L.; Joseph, C. A.; Maroney, M. J.; Dyer, R. B. *J. Am. Chem. Soc.* **2012**, *134*, 11108.
(18) Nann, T.; Ibrahim, S. K.; Woi, P.-M.; Xu, S.; Ziegler, J.; Pickett, C. J. *Angew. Chem., Int. Ed.* **2010**, *49*, 1574.
(19) Huang, J.; Mulfort, K. L.; Du, P.; Chen, L. X. *J. Am. Chem. Soc.* **2012**, *134*, 16472.
(20) Tseng, H.-W.; Wilker, M. B.; Damrauer, N. H.; Dukovic, G. *J. Am. Chem. Soc.* **2013**, *135*, 3383.
(21) Reynal, A.; Lakadamyali, F.; Gross, M. A.; Reisner, E.; Durrant, J. R. *Energy Environ. Sci.* **2013**, *6*, 3291.
(22) Varma, S.; Castillo, C. E.; Stoll, T.; Fortage, J.; Blackman, A. G.; Molton, F.; Deronzier, A.; Collomb, M.-N. *Phys. Chem. Chem. Phys.* **2013**, *15*, 17544.
(23) McCrory, C. C. L.; Uyeda, C.; Peters, J. C. *J. Am. Chem. Soc.* **2012**, *134*, 3164.
(24) Lakadamyali, F.; Reynal, A.; Kato, M.; Durrant, J. R.; Reisner, E. *Chem.—Eur. J.* **2012**, *18*, 15464.
(25) Artero, V.; Chavarot-Kerlidou, M.; Fontecave, M. *Angew. Chem., Int. Ed.* **2011**, *50*, 7238.
(26) Leung, C.-F.; Chen, Y.-Z.; Yu, H.-Q.; Yiu, S.-M.; Ko, C.-C.; Lau, T.-C. *Int. J. Hydrog. Energy* **2011**, *36*, 11640.
(27) Koops, S. E.; Durrant, J. R. *Inorg. Chim. Acta* **2008**, *361*, 663.
(28) Yu, W. W.; Qu, L.; Guo, W.; Peng, X. *Chem. Mater.* **2003**, *15*, 2854.
(29) Kaniyankandy, S.; Rawalekar, S.; Verma, S.; Palit, D. K.; Ghosh, H. N. *Phys. Chem. Chem. Phys.* **2010**, *12*, 4210.
(30) Kaniyankandy, S.; Rawalekar, S.; Ghosh, H. N. *J. Phys. Chem. C* **2012**, *116*, 16271.
(31) Costentin, C.; Drouet, S.; Robert, M.; Savéant, J.-M. *J. Am. Chem. Soc.* **2012**, *134*, 11235.
(32) Guttentag, M.; Rodenberg, A.; Kopelent, R.; Probst, B.; Buchwalder, C.; Brandstätter, M.; Hamm, P.; Alberto, R. *Eur. J. Inorg. Chem.* **2012**, *2012*, 59.
(33) Nippe, M.; Khnayzer, R. S.; Panetier, J. A.; Zee, D. Z.; Olaiya, B. S.; Head-Gordon, M.; Chang, C. J.; Castellano, F. N.; Long, J. R. *Chem. Sci.* **2013**, *4*, 3934.
(34) Sun, Y.; Sun, J.; Long, J. R.; Yang, P.; Chang, C. J. *Chem. Sci.* **2013**, *4*, 118.
(35) Wang, M.; Chen, L.; Sun, L. *Energy Environ. Sci.* **2012**, *5*, 6763.
(36) Thoi, V. S.; Sun, Y.; Long, J. R.; Chang, C. J. *Chem. Soc. Rev.* **2013**, *42*, 2388.
(37) Zhao, J.; Holmes, M. A.; Osterloh, F. E. *ACS Nano* **2013**, *7*, 4316.